ACS EARTH AND SPACE CHEMISTRY

http://pubs.acs.org/journal/aesccq

Article

Climate-Associated Changes in Mercury Sources in the Arctic Fjord Sediments

Ju Hyeon Lee, Sae Yun Kwon,* Hoin Lee, Seung-Il Nam, Jung-Hyun Kim, Young Ji Joo, Kwangchul Jang, Haryun Kim, and Runsheng Yin

Cite This: *ACS Earth Space Chem.* 2021, 5, 2398−2407

Read Online

ACCESS | Metrics & More | Article Recommendations | Supporting Information

ABSTRACT: Despite the large climatic fluctuations in the Arctic over the Holocene, the dominant mercury (Hg) sources and the potential changes in Hg sources associated with the climate remain unclear. Here, we use Hg isotopes to reconstruct changes in Hg sources and processes in two Svalbard fjord sediment cores spanning the Holocene. The Hg isotope ratios of the fjord sediment cores are similar to bedrock and Hg bound to terrestrial total organic carbon (TOC) but different from other sediment cores influenced by atmospheric Hg drawdowns via the sinking of marine particulate organic matter. The absence of significant Hg and TOC relationships indicates that bedrock erosion caused by glacier dynamics is the major Hg source to the fjord sediment rather than those bound to marine and terrestrial TOC. Measurable shifts in Hg sources are observed at regional cooling (4.3 ka) and during the Medieval Warm Period in the late Holocene. The negative shift in δ^{202}Hg (by −0.5‰) at 4.3 ka from baseline (∼10 ka) is consistent with the rapid increase in glacier-mediated physical and chemical erosions of bedrock. The significant positive shifts in δ^{202}Hg (by 0.5‰) in the late Holocene are explained by enhanced input of atmospheric Hg and its drawdown via the sinking of marine particulate organic matter and some anthropogenic influence, which suppressed the positive Δ^{199}Hg and Δ^{200}Hg shifts. This study suggests that Hg isotope ratios measured in sedimentary archives can be used to decipher climate and other local to global changes modifying Hg sources in the Arctic.

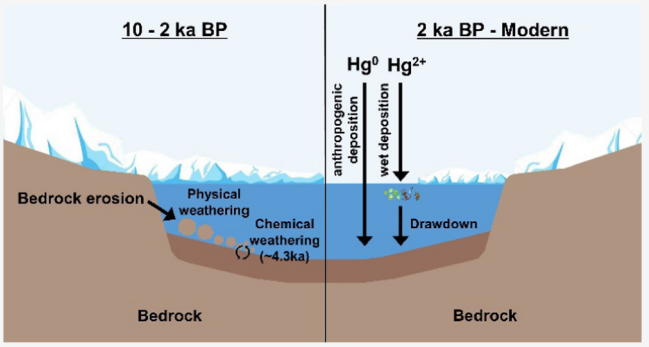

KEYWORDS: *stable isotope, Holocene, climate change, sediment core, proxy, reconstruction, Svalbard, Dicksonfjorden, Woodfjorden*

INTRODUCTION

While recent anthropogenic mercury (Hg) emissions have received much attention due to the toxicity of Hg to the ecosystem and human health,[1] studies of natural sources and processes leading to long-term changes in Hg in geochemical reservoirs have been relatively limited. Constraining the natural levels and factors governing natural Hg sources and processes are important for evaluating modern anthropogenic influences and for predicting future changes in the Hg cycle. Reconstructions of Hg deposition history in lake sediment cores have shown 3−5-fold increases in Hg accumulation rates since industrialization.[2,3] Historic volcanic eruptions have resulted in 5−12-fold increases in Hg accumulation rates in ice cores relative to the background.[4] In addition to these dramatic perturbations, responses to gradual and dynamic changes such as climate change can provide insights into how natural processes modify Hg sources, transport, and fate in ecosystems.[5]

The Arctic underwent a profound glacial−interglacial transition during the Holocene.[6] A compilation of biogeochemical measurements in lake, fjord, and marine sediment cores from the Svalbard archipelago has revealed sequences of small- to large-scale climatic events including (1) the Holocene Thermal Maximum (HTM) resulting in glacial minimum in the early-to-middle Holocene, (2) several regional cooling events in the middle-to-late Holocene, and (3) the Medieval Warm Period in the late Holocene.[6] To date, only a few studies have investigated changes in Hg sources and processes over the Holocene in Arctic lake[7−9] and marine sediment cores.[10] By coupling total organic carbon (TOC) and stable carbon isotopes ($\delta^{13}C_{org}$) as biogeochemical proxies, peaks in sediment Hg concentration have been explained by either increased runoff of soil Hg or enhanced primary productivity leading to algal Hg scavenging. Unfortunately, the interpretation of more complex and/or subtle variations in Hg has been

Received: April 12, 2021
Revised: August 5, 2021
Accepted: August 9, 2021
Published: August 23, 2021

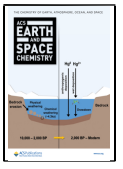

https://doi.org/10.1021/acsearthspacechem.1c00095
ACS Earth Space Chem. 2021, 5, 2398−2407

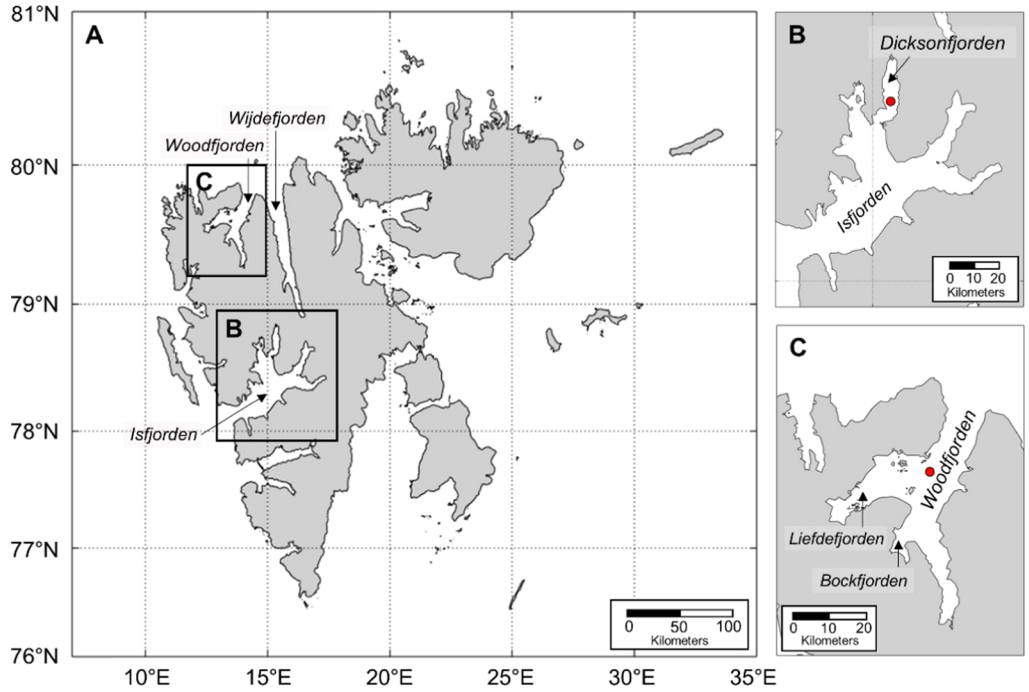

Figure 1. Map of sampling locations in Svalbard (A): Dicksonfjorden (B) and Woodfjorden (C).

difficult due to the absence of proxies that can capture changes among various sources and biogeochemical processes of Hg.

The measurement of Hg isotopes may be an effective tool for understanding changes in Hg sources in the Arctic. Mercury isotopes undergo mass-dependent fractionation (MDF; δ^{202}Hg) and mass-independent fractionation during environmental cycling, which provide multidimensional information about the Hg biogeochemistry. Hg-MDF occurs via almost all biogeochemical processes involved in the Hg cycle[11,12] and Hg-MIF occurs during specific processes. MIF of odd-mass isotopes (MIF_{odd}; Δ^{199}Hg, Δ^{201}Hg) is caused primarily via aqueous inorganic (Hg^{2+}) photoreduction and methylmercury (MeHg) photodegradation,[13] and MIF of even-mass isotopes (MIF_{even}; Δ^{200}Hg) is thought to be caused by elemental Hg (Hg^0) photo-oxidation in the atmosphere.[14] Given the limited processes resulting in MIF_{odd}, Δ^{199}Hg in sedimentary archives have been used to reconstruct anthropogenic Hg sources in modern history[15,16] and the influence of large igneous provinces (LIPs) Hg emissions during critical events in geological history.[17−19] A recent evaluation of Hg isotope ratios in lake sediment cores across North America has also shown that Δ^{200}Hg can be used to distinguish between the relative input of atmospheric (positive Δ^{200}Hg) and watershed-derived Hg sources (near-zero Δ^{200}Hg).[16] In regard to climate-associated changes in Hg processes, Masbou et al.[20] and Yin et al.[21] reported temporal increases in Δ^{199}Hg in the Arctic ringed seal (1988−2002) and in the Tibetan lake sediment core (1800−2005), respectively, in association with gradual loss of ice cover. These studies have suggested that increased Hg^{2+} and MeHg photoreduction within the water column, resulting in positive Δ^{199}Hg in the remaining Hg, prior to bioaccumulation and sediment deposition, is responsible for the temporal Δ^{199}Hg increase. As for Hg sources, recent studies have reported large δ^{202}Hg and Δ^{199}Hg and subtle Δ^{200}Hg variations in snow, glacial and snowpack meltwater, and peat core,[22−24] suggesting the potential utility of Hg isotopes for identifying changes in Hg sources in the Arctic ecosystem.

Here, we measured the concentrations and isotope ratios of Hg in two age-dated fjord sediment cores collected from Svalbard, Arctic, which has a long history of scientific observations and reconstructions of changes in fjord glacial and terrain landforms and biogeochemical processes.[6] By comparing with a suite of biogeochemical measurements (TOC, $\delta^{13}C_{org}$, neodymium isotope; ε_{Nd}) conducted previously in the same fjord sediment cores, we aim to (1) identify dominant Hg sources and transport pathways into Svalbard fjords, (2) evaluate temporal changes in Hg sources, and (3) verify which particular changes are associated with climatic events over the Holocene relative to other local to global changes (i.e., anthropogenic activities). We expect that this study would aid the identification of potential opportunities and challenges of using Hg isotopes as a complementary tool for assessing changes in Hg sources in the Arctic.

MATERIALS AND METHODS

Site Description. Sediment cores were collected from Dicksonfjorden and Woodfjorden, Svalbard (Figure 1). Dicksonfjorden is located in a northern tributary of Isfjorden, one of the largest fijord sytems in Svalbard (Figure 1B). Dicksonfjorden is 30 km long and 7 km wide, with a catchment area of 1013 km^2. The maximum water depth is 123 m in the southern part of Dicksonfjorden. Woodfjorden is the fourth-longest fjord in the Svalbard (Figure 1C), which is 65 km long and 10 km wide, with a maximum water depth of 200 m in the central part of Woodfjorden.[25] The glaciers in Dicksonfjorden all terminate on land and there are several tidewater glaciers in Woodfjorden.[26] Two sediment cores were selected from two fjord systems due to the differences in the onset and the extent of glacier activities during the HTM and the regional cooling events,[6] which may modify the relative influence of atmospherically deposited Hg and Hg sources originating from glacier melting and bedrock erosion over the Holocene.

https://doi.org/10.1021/acsearthspacechem.1c00095
ACS Earth Space Chem. 2021, 5, 2398−2407

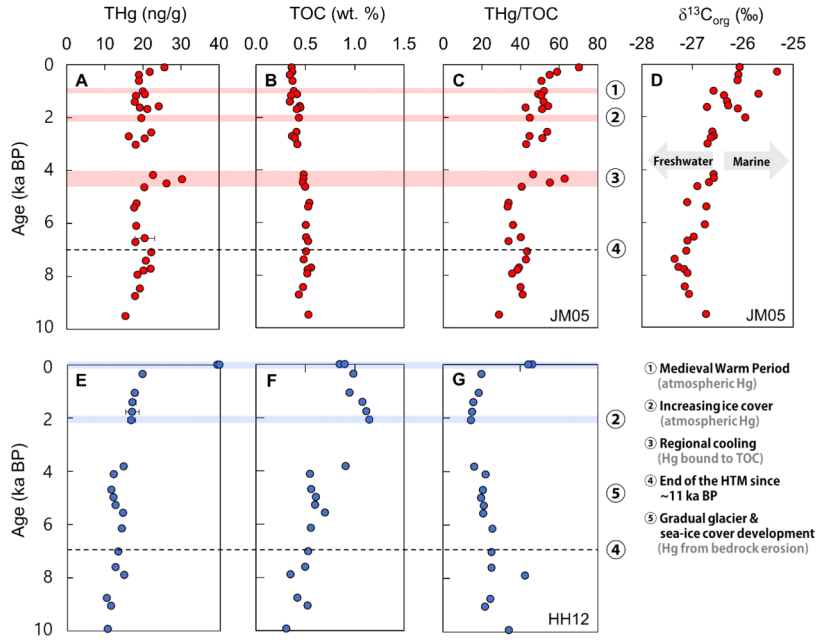

Figure 2. Temporal variations in THg concentration, TOC, and THg/TOC ratios of JM05 (A, C) and HH12 (E−G) measured in this study and TOC (B; JM05) and $\delta^{13}C_{org}$ (D; JM05) reported in Joo et al.[27] Reproduced from Joo et al.[27] under a Creative Commons CC BY-NC 4.0 license Copyright 2019 Norwegian Polar Institute.

Sample Collection. Sediment cores in Dicksonfjorden (JM05-046-GC; 78°40.50′N, 15°18.89′E; water depth of 88 m) and Woodfjorden (HH12-964-GC; 79°39.04′N, 13°45.3′E; water depth of 173 m) were retrieved using a gravity corer during cruises of RV Jan Mayen/Helmer Hanssen of UiT, The Arctic University of Norway in Tromsø in 2005 and 2012, respectively. JM05-046-GC (referred to as JM05) is 299 cm long, spanning the last 10.8 ka.[27] HH12-964-GC (referred to as HH12) is 334 cm long with a bottom age of 13.3 ka.[25] Each core was cut into 1 m sections and kept at 4 °C in a core repository. Sediments were further sampled at 2 cm intervals for JM05 and 5 cm intervals for HH12 and freeze-dried and powdered before analyses. The lithologies of JM05 and HH12 are described in Jang et al.[28] and Joo et al.[27,29] and summarized in Table S1. The TOC, $\delta^{13}C_{org}$, ε_{Nd}, and ages of the two cores were reported previously[27,28] and are summarized in Table S2.

Hg Concentration and Isotopic Composition Analyses. Subsamples from the two cores (JM05; n = 33, HH12; n = 20) were selected to measure total Hg (THg) concentrations and Hg isotope ratios at the Environmental Health Assessment Laboratory, Pohang University of Science and Technology, South Korea. THg concentrations were directly analyzed by a Nippon Instruments MA-3000 Hg analyzer. Standard reference material (TORT-3; lobster, MESS-4; marine sediment) and sample duplicates were included for quality control and quality assurance. Recoveries ranged between 88 and 96% (n = 23) for TORT-3 and between 81 and 88% (n = 7) for MESS-4, and the relative standard deviations of sample duplicates were within 13%.

Mercury isotope ratios were determined by a Nu-Plasma III multicollector inductively coupled plasma mass spectrometer (MC-ICP-MS). Approximately 0.4−1.5 g of sample was loaded into a double-stage thermal combustion furnace to release all Hg^0 from the samples, and the released Hg^0 was preconcentrated into a 1% $KMnO_4$ (in 10% H_2SO_4) solution. The preconcentration process yielded Hg recoveries of 82−116% for the samples, 86−115% for TORT-3 (n = 7), and 81−124% for MESS-4 (n = 2), according to THg concentrations of the trapping solutions measured by a cold vapor atomic fluorescence spectrometer (Brooks Rand). The trap solutions were neutralized with NH_2-OH-HCl, diluted to 1−3 ng/mL Hg, and introduced to the MC-ICP-MS via a gas−liquid separator and by continuously reducing Hg^{2+} with 2% $SnCl_2$. Instrumental mass bias was corrected using an internal thallium standard (NIST SRM 997), introduced via a desolvating nebulizer (CETAC Aridus3) and by bracketing each sample with NIST SRM 3133 with the same matrices and THg concentrations. MDF is reported as δ^{202}Hg (‰) referenced to NIST SRM 3133[29]

$$\delta^{202}\mathrm{Hg} = \{[(^{202}\mathrm{Hg}/^{198}\mathrm{Hg})_{\mathrm{sample}}/(^{202}\mathrm{Hg}/^{198}\mathrm{Hg})_{\mathrm{NIST3133}}] - 1\} \times 1000 \quad (1)$$

MIF is reported as Δ^{199}Hg, Δ^{200}Hg, and Δ^{201}Hg (‰) and calculated using the following equations[30]

$$\Delta^{199}\mathrm{Hg} = \delta^{199}\mathrm{Hg} - (\delta^{202}\mathrm{Hg} \times 0.2520) \quad (2)$$

$$\Delta^{200}\mathrm{Hg} = \delta^{200}\mathrm{Hg} - (\delta^{202}\mathrm{Hg} \times 0.5024) \quad (3)$$

$$\Delta^{201}\mathrm{Hg} = \delta^{201}\mathrm{Hg} - (\delta^{202}\mathrm{Hg} \times 0.7520) \quad (4)$$

Analytical uncertainty at 2 standard deviation (2SD) is estimated based on replicate analyses of either NIST RM 8610 (known as UM-Almaden; n = 42), TORT-3 (n = 4) or MESS-4 (n = 2) (Table S3). Hg isotope ratios of NIST RM 8610 were −0.56 ± 0.08‰ for δ^{202}Hg, −0.02 ± 0.04‰ for Δ^{199}Hg, and 0.00 ± 0.04‰ for Δ^{200}Hg. Hg isotope ratios of TORT-3 were 0.10 ± 0.10‰ for δ^{202}Hg, 0.62 ± 0.10‰ for Δ^{199}Hg, and 0.06 ± 0.02‰ for Δ^{200}Hg, and Hg isotope ratios of MESS-4 were −2.07 ± 0.03‰ for δ^{202}Hg, 0.04 ± 0.06‰ for Δ^{199}Hg, and 0.01 ± 0.03‰ for Δ^{200}Hg, both similar to those reported by Blum and Johnson.[31] We used TORT-3 to report 2SD as it had the largest analytical uncertainty.

https://doi.org/10.1021/acsearthspacechem.1c00095
ACS Earth Space Chem. 2021, 5, 2398−2407

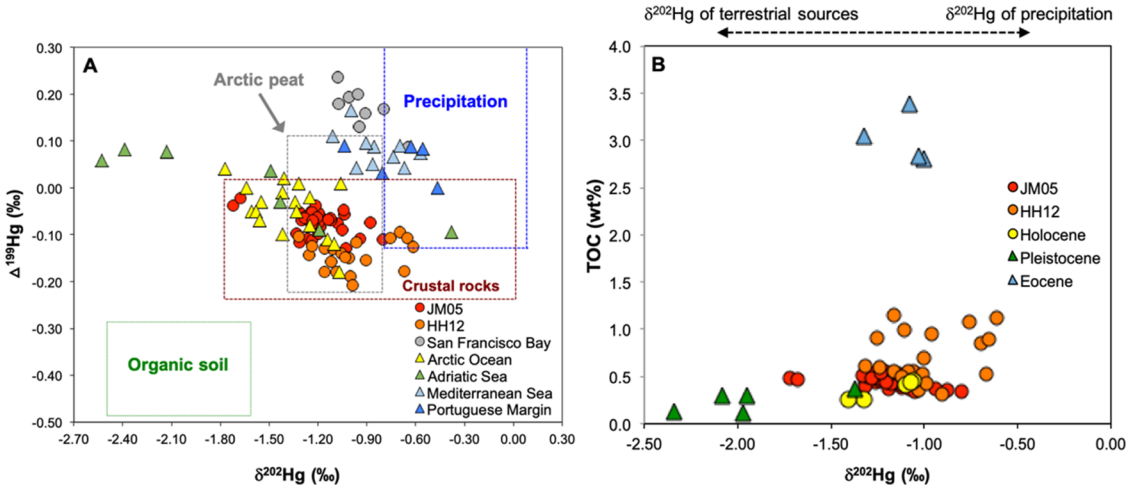

Figure 3. (A) δ^{202}Hg and Δ^{199}Hg of JM05 and HH12 and other preindustrial coastal[48] and marine sediment cores.[10,32,33,46] The boxes represent the ranges of δ^{202}Hg and Δ^{199}Hg of organic soil,[51] Arctic peat,[22,42] crustal rocks,[44] and precipitation.[47−50] (B) δ^{202}Hg and TOC of JM05 and HH12 and the Holocene, Pleistocene, and Eocene sediments collected from the Arctic Ocean.[10] Reproduced with permission from Gleason et al.[10] Copyright 2017 Elsevier; Foucher and Hintelmann[32] Copyright 2009 American Chemical Society; Mil-Homens et al.[33] Copyright 2013 Elsevier; Gehrke et al.[46] Copyright 2009 Elsevier; Gratz et al.[48] Copyright 2010 American Chemical Society.

RESULTS AND DISCUSSION

Temporal Variations in THg, TOC, and THg/TOC. The fjord sediment cores collected from two different locations of Svalbard exhibited minor temporal variations in THg concentration (Figure 2A,E). The THg concentrations of the JM05 and HH12 cores ranged between 15.5 and 30.3 ng/g (Figure 2A) and between 10.3 and 39.9 ng/g (Figure 2E), respectively, which are within the ranges of other preindustrial marine sediment cores.[10,32,33] By setting the baseline as the average THg concentration of the three bottom samples (10.8 ng/g for HH12 and 17.6 ng/g for JM05), we found that the HH12 core exhibited a 3.7-fold peak in THg at the surface, and the JM05 core exhibited a 1.7-fold peak in THg at 4.3 ka. The magnitude of THg increase on the surface layer of HH12, reflecting >1950 AD (0 cm depth; Table S5), is consistent with the degree of anthropogenic enrichment (3−5-fold increase) reported in lake sediment cores at various locations of the world.[2,3] The surface layer of JM05, which reflects ∼1840 AD (4 cm depth; Table S4) and has a low time resolution, shows a slight increase in THg possibly due to the anthropogenic influence. Modern-day anthropogenic activities appear to have a higher Hg influence in Woodfjorden (HH12) relative to Dicksonfjorden (JM05) due to its proximity to old mines located on the northwestern side of Svalbard.[34,35] Alternatively, the uppermost layer of HH12 reflecting a more recent period relative to JM05 may explain the higher degree of anthropogenic Hg enrichment in HH12.

The ranges of TOC in JM05 and HH12 are 0.34−0.56 wt % (Figure 2B) and 0.31−1.15 wt % (Figure 2F), respectively. These values are similar to those observed in the Arctic marine sediment cores spanning the Holocene (0.26−0.45 wt %)[10] and current coastal (0.29−0.93 wt %) and open ocean (0.23−0.67 wt %) sediments compiled by Xue et al.[36] Regarding the temporal variations, the JM05 core exhibited a minor declining temporal trend in TOC toward the modern-day period. The HH12 core showed an overall increasing trend and a slight decreasing trend beginning at 2 ka and onward. The greater TOC input to HH12 relative to JM05 can be explained by the influence of glaciofluvial rivers, which transport some sediment and TOC from inner Woodfjorden and those nearby Bockfjorden and tidewater glaciers in Liefdefjorden (Figure 1C).[26]

THg/TOC ratios in sediments have been used to determine whether variations in THg are driven by changes in the organic matter input.[18,19,37] We found that the THg/TOC of JM05 (29.0−70.5 ng/g/%; Figure 2C) and HH12 (14.6−46.2 ng/g/%; Figure 2G) has opposite temporal trends relative to TOC. The JM05 core showed an overall increasing trend in THg/TOC and a peak at 4.3 ka, which matches well with the peak in THg. In HH12, the THg/TOC showed small reductions until 2 ka and an increasing trend since then. The minor temporal variations in THg and the opposite trends between TOC and THg/TOC indicate that Hg bound to TOC is unlikely the major source or transport pathway of Hg to our fjord systems. Joo et al.,[27] based on the $\delta^{13}C_{org}$ in the JM05 core, suggested that a large proportion of TOC is allochthonous, reflecting TOC derived from the terrestrial environment rather than those produced within the fjord. The absence of significant positive relationships between THg and TOC in both sediment cores (JM05; $r^2 < 0.01$, HH12; $r^2 = 0.20$, both $p > 0.05$) is in contrast with many previous studies, which observed significant relationships in lakes,[38,39] lacustrine,[40] and marine sediment cores[41] spanning the Holocene. It is possible that, while TOC is derived from the terrestrial environment, Hg may have originated from a different source. Alternatively, Hg was not bound to terrestrial organic matter during transport from land. In the following sections, we examine Hg isotope ratios in the same sections of the sediment cores to understand the dominant sources and transport pathways of Hg into the fjords (Sources and Transport Pathways of Hg Into Fjord Sediment section) and to evaluate processes governing the spatiotemporal variability in Hg isotope ratios (Temporal Variations in Hg Isotope Ratios section).

Sources and Transport Pathways of Hg into Fjord Sediment. The ranges of δ^{202}Hg, Δ^{199}Hg, and Δ^{200}Hg of JM05 are −1.72 to −0.80‰, −0.13 to −0.02‰, and −0.03 to 0.05‰, respectively (Table S4). The ranges of δ^{202}Hg, Δ^{199}Hg, and Δ^{200}Hg of HH12 are −1.32 to −0.61‰, −0.21 to −0.09‰, and −0.03 to 0.02‰, respectively (Table S5). As

https://doi.org/10.1021/acsearthspacechem.1c00095
ACS Earth Space Chem. 2021, 5, 2398−2407

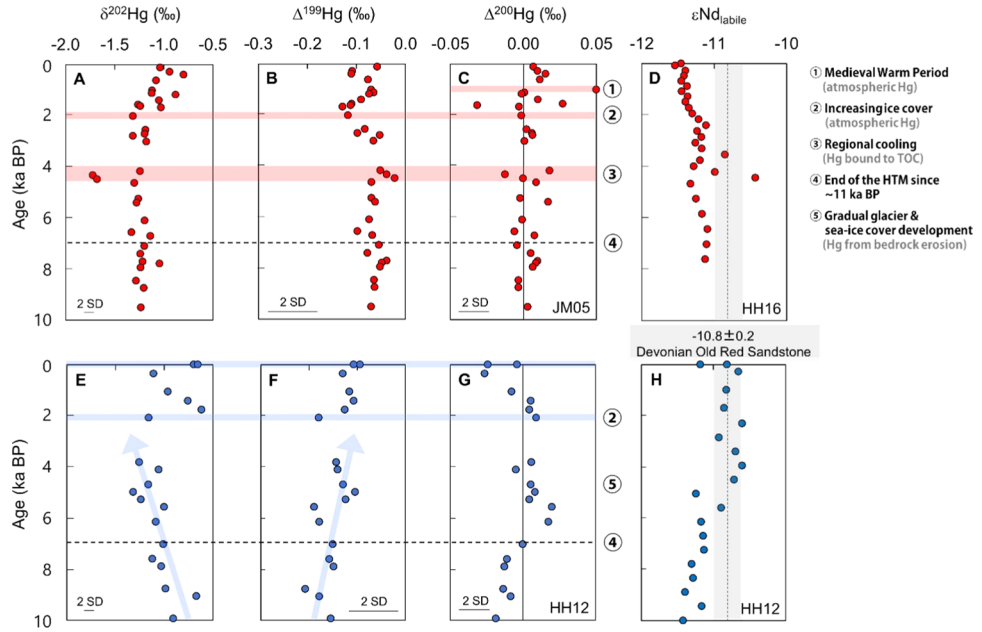

Figure 4. Temporal variations of δ^{202}Hg, Δ^{199}Hg, and Δ^{200}Hg in JM05 (A−C) and HH12 (E−G) measured in this study and labile ε_{Nd} (D; gravity core collected from Dicksonfjorden in 2016, H; HH12) reported in Jang et al.[28] (Table S2). Reproduced with permission from Jang et al.[28] Copyright 2020 Elsevier.

illustrated in Figure 3A, the δ^{202}Hg and Δ^{199}Hg of two fjord sediment cores are similar to the Arctic marine sediment cores spanning the Holocene[10] and are within the ranges of the Arctic peat[24,42] and crustal rocks.[43,44] The Δ^{199}Hg of both fjord cores are more negative than those of other low-latitude coastal (San Francisco Bay)[45] and marine sediment cores reflecting preindustrial periods (based on the age constrained from the individual studies; Mediterranean Sea;[46] Portuguese Margin[33]) and more positive in δ^{202}Hg compared to marine sediment cores collected from the Adriatic Sea.[32] Marine sediments are thought to receive Hg primarily via precipitation and riverine transport,[32,47] with each source having different δ^{202}Hg and Δ^{199}Hg. As shown in Figure 3A, the positive Δ^{199}Hg observed in coastal (San Francisco Bay)[45] and marine sediment cores (Mediterranean Sea;[46] Portuguese Margin[33]) compiled from various locations are similar to the values of precipitation collected from remote regions.[47−50] Marine sediment cores from the Adriatic Sea are known to receive significant amounts of Hg via riverine and coastal transport (Soča and Isonzo River and Gulf of Trieste) and show highly negative δ^{202}Hg,[32] consistent with the negative δ^{202}Hg observed in organic soil.[51]

The differences in preindustrial sediment Hg isotope ratios observed between the Arctic (this study and Gleason et al.[10]) and low-latitude environments suggest that the relative importance of Hg sources may differ depending on the geographic location, as suggested by Li et al.[52] Even within the Arctic, the δ^{202}Hg versus TOC pattern observed among sediments reflecting different geological periods indicates that the relative importance of Hg sources and transport pathways may vary with the climatic conditions. As illustrated in Figure 3B, Gleason et al.[10] suggested that Arctic marine sediment sections reflecting periods of widespread sea ice cover during the glacial periods in the Pleistocene (2580−11.7 kya) received relatively little Hg input via periodic terrestrial runoff. Such climatic conditions have been used to explain the low THg, TOC, and δ^{202}Hg, consistent with the δ^{202}Hg of organic soil.[51]

The Eocene (56−33.9 mya), by contrast, is known for its warm climate including the Paleocene−Eocene Thermal Maximum and high marine productivity, which has been suggested to cause drawdowns of Hg accumulated in marine particulate organic matter (i.e., particles, plankton), resulting in high-sediment THg and TOC. The δ^{202}Hg of the Eocene sediments were attributed to the effect of Hg in precipitation, which has a higher δ^{202}Hg relative to terrestrial Hg sources.[10] The somewhat intermediate TOC and δ^{202}Hg in the Holocene sediment were explained by the alternating warm and cool periods over the Holocene, causing the introduction of both terrestrial and atmospheric Hg sources.[10]

Despite the overlapping δ^{202}Hg and TOC ranges between our Holocene fjord sediment cores and the Holocene marine sediment cores (Figure 3B), multiple lines of evidence suggest that Hg liberated from bedrock, in addition to terrestrial and atmospheric Hg sources bound to TOC, act as the dominant Hg source to our fjord sediment cores. Among the potential Hg sources compiled here, the Hg isotope ratios of the fjord sediment cores overlapped with the crustal rocks[44] and Arctic peat (Figure 3A).[22,42] The main bedrock of Dicksonfjorden and Woodfjorden is the Devonian Old Red Sandstone (Table S1), and we observed similar δ^{202}Hg, THg, and TOC between the fjord sediment cores and various types of sandstones collected from California Coast Ranges, U.S.A. (δ^{202}Hg; −1.21 to −0.53‰, THg; 31.5−88.0 ng/g, TOC; 0.08−0.35 wt %, all n = 6) but not with other rock types measured in the study (e.g., serpentinite, blueschist).[43] The overlapping ranges in Hg isotope ratios between the fjord sediment cores and the Arctic peat, reflecting atmospheric Hg^0 sequestered into vegetation prior to decomposition,[53] and the significantly negative Δ^{199}Hg of the fjord sediment cores indicate that terrestrial Hg may have also contributed as a source to the studied sites. With regard to Δ^{200}Hg, JM05 and HH12 displayed similar values with organic soil (average −0.03 ± 0.03‰, n = 44)[42,51,54] and sedimentary rocks (average 0.00 ± 0.01‰, n = 21).[31]

https://doi.org/10.1021/acsearthspacechem.1c00095
ACS Earth Space Chem. 2021, 5, 2398−2407

Our results are consistent with recent studies, which suggested that Hg liberated from bedrock is the primary Hg source to Svalbard fjord sediments. Kim et al.[55] observed significant positive relationships between detrital metals derived from bedrock (zirconium, titanium, hafnium) and THg in surface sediments of Dicksonfjorden and Wijdefjorden, located just east of Woodfjorden (Figure 1). Jang et al.[28] reported comparable ε_{Nd}, an indicator for continental weathering and sedimentary processes, between the Devonian Old Red Sandstone (detrital fraction; −13.6 ± 0.3, labile fraction; −10.8 ± 0.2) and the Holocene sediment cores collected from Dicksonfjorden (−13.5 ± 0.3, −11.2 ± 0.2) and Woodfjorden (−13.6 ± 0.5, −11.2 ± 0.3). Nevertheless, there is a major difference between our study and that of Kim et al.,[55] who reported a significant positive relationship between THg and TOC in the Dicksonfjorden surface sediments. The significantly positive THg and TOC relationships observed by Kim et al.[55] in the surface sediments may be explained by the release of Hg from bedrock erosion and sequestration by organic matter in the sediment. Alternatively, while the rapid deglaciation occurring in modern-day Svalbard is responsible for chemical erosion of bedrock and release of organic matter available for Hg sequestration and transport into fjord sediment,[55] the effect of glaciation leading to physical erosion of bedrock and ice rafting may have been more pronounced during the Holocene (this study). This hypothesis is consistent with the lithology of JM05,[27] which revealed a large proportion of coarse grain sediments particularly during the regional cooling periods. While further study is required to verify Hg transport pathways, our results together with previous studies suggest that bedrock erosion supplies the majority of Hg into Svalbard fjord systems.

Temporal Variations in Hg Isotope Ratios. We couple ε_{Nd} and $\delta^{13}C_{org}$ measured previously either in the same core or cores collected from the same location (Table S2) to evaluate sources and processes governing the spatiotemporal variability in Hg isotope ratios (Figure 4). In JM05, we observed small variations in Hg isotope ratios between the early Holocene and 2.0 ka, except for significant negative δ^{202}Hg (by 0.46‰, >2SD) and small positive Δ^{199}Hg shifts (by 0.04‰, <2SD) at 4.3 ka relative to the baseline (average Hg isotope ratios of three bottom samples). Between 2.0 ka and the modern-day period, the δ^{202}Hg exhibited significant positive shifts (by 0.20‰) and the Δ^{199}Hg and Δ^{200}Hg showed minor changes relative to the baseline. A significant positive Δ^{200}Hg shift (by 0.05‰, >2SD) was also detected at 1.0 ka. In HH12, we observed significantly more positive δ^{202}Hg (−0.85‰) and negative Δ^{199}Hg (−0.18‰) baselines relative to JM05 (δ^{202}Hg; −1.24‰, Δ^{199}Hg; −0.07‰). There was a significant decreasing trend in δ^{202}Hg (by 0.31‰) and minor increasing trends in Δ^{199}Hg and Δ^{200}Hg between the early Holocene and 2.0 ka relative to the baseline. Between 2.0 ka and the modern-day period, significant positive shifts in the δ^{202}Hg (by 0.16‰) and Δ^{199}Hg (by 0.09‰) were observed.

Based on the temporal variations in the Hg isotope ratios, we divide changes in Hg sources into two main periods: 10−2 ka and 2 ka−modern-day. To explain JM05 first, the overall consistent negative δ^{202}Hg and Δ^{199}Hg and the small TOC and THg variations between the early Holocene and 2.0 ka suggest that the bedrock erosion remained as the major Hg source to JM05. The negative δ^{202}Hg and positive Δ^{199}Hg peaks at 4.3 ka coincide with many previous studies, which reported episodic increases in sedimentation rates across Svalbard fjords caused by glacier-mediated bedrock erosion during the regional cooling.[6] The profile of ε_{Nd}, reflecting the labile fractions from a Dicksonfjorden sediment core, also exhibited a peak at 4.3 ka (Figure 4D). Jang et al.[28] attributed this phenomenon to rapid glacier advancement in Dicksonfjorden during the regional cooling, resulting in physical erosion of bedrock and exposure of substrates available for chemical weathering of labile materials. The concurrent peaks in THg and THg/TOC and not in TOC (Figure 2A−C) also suggest that Hg derived from both physical and chemical bedrock erosion increased rapidly relative to Hg bound to TOC during the regional cooling.

In contrast to JM05, HH12 exhibited gradual δ^{202}Hg and Δ^{199}Hg changes between the early Holocene and 2 ka from more negative Δ^{199}Hg baseline relative to JM05. Given that Woodfjorden receives sediment and TOC from the glaciofluvial rivers,[26] the negative δ^{202}Hg and Δ^{199}Hg values at the bottom core may indicate that Hg bound to terrestrial TOC may have contributed as the primary source in HH12 in the early Holocene. The differences in the geographical location and glacier dynamics between two fjord systems may explain the point in time when the relative contribution of Hg sources has shifted during the Holocene. Farnsworth et al.[6] reported that the ice-free period in northern Svalbard was much longer than central Svalbard during the early-to-middle Holocene. Relative to Dicksonfjorden, which experienced rapid glacier advancement, the slow glacier development, resulting in both physical and chemical erosions of bedrock, in Woodfjorden may explain the gradual modifications in δ^{202}Hg and Δ^{199}Hg to values similar to the peaks observed at 4.3 ka in JM05 (Figure 4A,B,E,F). This is supported by the gradual increase in the ε_{Nd} to values identical to the Devonian Old Red Sandstone in HH12 (Figure 4H).

The significant positive shifts in δ^{202}Hg and small relative increases in THg between 2 ka and the modern-day period, except at the uppermost layer in JM05 and HH12, suggest that the contribution of Hg sourced from bedrock has decreased relative to the increases in other Hg sources in the late Holocene. In fact, 2 ka is an important period in Svalbard, marked by the beginning of extensive ice cover near fjord shores and moraine stabilization,[27,56] which may suppress glacier-mediated bedrock erosion and the Holocene minimum in fjord sedimentation rates.[57] Multiple biogeochemical records have suggested that 1−0.4 ka is known as the Medieval Warm Period in which Dicksonfjorden and Woodfjorden have experienced the inflow of Atlantic water and increased marine primary productivity.[27,58,59]

Based on these climatic changes as well as significant temporal increases in δ^{202}Hg and $\delta^{13}C_{org}$ but not in Δ^{199}Hg and Δ^{200}Hg during the late Holocene (Figure 4), we propose that the mixture of two different Hg sources explains the observed trends in Hg and C isotope ratios. First, we think that the relative contribution of marine particulate organic matter, which has more positive δ^{202}Hg and $\delta^{13}C_{org}$ compared to bedrock and terrestrial sources as well as freshwater particulate organic matter, has increased in JM05 and HH12. Motta et al.[60] observed more positive δ^{202}Hg relative to bedrock and positive Δ^{199}Hg and Δ^{200}Hg in precipitation (δ^{202}Hg; 0.07 ± 0.08‰, Δ^{199}Hg; 0.33 ± 0.24‰, Δ^{200}Hg; 0.14 ± 0.05‰, n = 7), marine particles (δ^{202}Hg; −0.12 ± 0.13‰, Δ^{199}Hg; 0.16 ± 0.09‰, Δ^{200}Hg; 0.06 ± 0.03‰, n = 11), and planktons (δ^{202}Hg; −0.14 ± 0.21‰, Δ^{199}Hg; 0.85 ± 0.51‰, Δ^{200}Hg; 0.07 ± 0.08‰, n = 33) in the Central Pacific Ocean and

https://doi.org/10.1021/acsearthspacechem.1c00095
ACS Earth Space Chem. 2021, 5, 2398−2407

suggested that Hg^{2+} introduced via precipitation and those adsorbed and/or bioaccumulated into marine particles and planktons are retained throughout the water column during sediment suspension. Although only one core section at 1 ka displayed a significant positive $\Delta^{200}Hg$ (0.05‰), this is noteworthy as only a few environmental samples influenced by atmospheric Hg^{2+} (i.e., precipitation, seawater, plankton, fish) have positive $\Delta^{200}Hg$.[12] The reason that we propose marine particulate organic matter as a source, rather than direct precipitation input, is that TOC, despite the Holocene minimum in the sedimentation rate[57] and moraine stabilization,[27,56] showed only minor temporal reductions during this period. The increased marine primary productivity during the Medieval Warming Period would have supplied autochthonous TOC, as revealed by the positive shifts in $\delta^{13}C_{org}$ (Figure 2D), resulting in atmospheric Hg^{2+} drawdown into the fjord sediment.

Second, the fact that the $\Delta^{199}Hg$ and $\Delta^{200}Hg$ did not exhibit concurrent temporal increases via the sinking of marine particulate organic matter indicates that an additional Hg source, with negative to near-zero $\Delta^{199}Hg$ and $\Delta^{200}Hg$, has diluted the marine Hg source. Among the potential Hg sources, precipitation and marine particulate organic matter, as discussed above, are characterized by more positive $\delta^{202}Hg$ relative to bedrock and significant positive $\Delta^{199}Hg$ and $\Delta^{200}Hg$. Although the Arctic peat has a similar $\delta^{202}Hg$ range with the bedrock and near-zero $\Delta^{200}Hg$,[53] the wide ranges in $\Delta^{199}Hg$ (both positive and negative) and the positive $\delta^{13}C_{org}$ shifts toward the marine source suggest that Hg released from peat is unlikely to be an important source. The positive shifts in $\delta^{13}C_{org}$ and highly negative $\delta^{202}Hg$ in organic soil also indicate that runoff of soil-bound Hg cannot explain the observed temporal changes in Hg and C isotope ratios.

While the onset of historical anthropogenic activities dates back to only ~0.4 ka,[61] we think that gradual increases in the global anthropogenic Hg^0 emissions have enhanced the regional atmospheric Hg level available for deposition and begun to suppress the positive $\Delta^{199}Hg$ and $\Delta^{200}Hg$ shifts in the modern-day period. Sun et al.[62] estimated the isotopic end member for anthropogenically emitted Hg^0, reflecting those emitted prior to 1850s via silver and ore mining and reported a median $\delta^{202}Hg$ of −0.91‰ (−1.49 to −0.49‰) and near-zero $\Delta^{199}Hg$ (−0.04 to 0.04‰) and $\Delta^{200}Hg$. The estimated isotopic end member for anthropogenically emitted Hg matches well with the $\delta^{202}Hg$ (−1.04 to −0.80‰, n = 3), $\Delta^{199}Hg$ (−0.11 to −0.06‰, n = 3), and $\Delta^{200}Hg$ (0.01−0.02‰, n = 3) in the uppermost part of JM05 (>1560 AD) and the $\delta^{202}Hg$ (−1.11 to −0.65‰, n = 3), $\Delta^{199}Hg$ (−0.13 to −0.09‰, n = 3), and $\Delta^{200}Hg$ (−0.03 to 0.00‰, n = 3) in the uppermost layers of HH12 (>1595 AD). Similar temporal trends in Hg isotope ratios have been reported from many remote lake sediment cores, trending toward the anthropogenic Hg source endmember.[15,16] Our hypothesis is supported by substantial mining-related Hg emissions around the world[57] as well as anthropogenic Hg enrichments reported in lake sediment[59] and peat cores[56] since 0.4 ka. Li et al.[52] also reported significant historical anthropogenic Hg emissions related to mining, deforestation, and biomass burning and consistent anthropogenic Hg enrichments from background level to preindustrial period (~1450 AD) across wide geographic regions. Historical records have also revealed local mining activities in the northwest Svalbard since 1905,[34] which may explain the ~3.7-fold increase in THg in HH12 relative to the baseline. The absence of a large TOC increase and low sedimentation rate further indicate that Hg sourced from the atmosphere likely played an important role during this period. All in all, we suggest that Hg^{2+} sourced from precipitation and those bioaccumulated into marine particulate organic matter served as the dominant source and Hg^0 emitted from anthropogenic activities have contributed to the suppression of $\Delta^{199}Hg$ and $\Delta^{200}Hg$ between 2 ka and the modern-day period.

Implications for Past and Future Global Change. The reconstruction of Hg sources in the Svalbard fjord sediment cores suggests that climatic changes modifying glacier dynamics and bedrock erosion are the primary sources and processes leading to Hg input over the Holocene. The relative contribution of Hg sourced from the atmosphere increases in the late Holocene with increased marine primary productivity in the Medieval Warm Period, which causes drawdown of precipitation of Hg^{2+}, and local to global increases in anthropogenic Hg^0 emissions. Our study is different from previous studies, which measured Hg isotope ratios in natural archives to understand historical[63] and modern-day anthropogenic influences[15,16] and to identify critical events in geological history.[17−19] We show that Hg isotopes, coupled with other biogeochemical proxies, can be used as a complementary tool for deciphering between climate and other local to global changes resulting in temporal modifications in Hg sources. With the acceleration of glacier retreatment in Svalbard fjords[55] and other Arctic regions,[64] we expect that the Hg isotope profiles established in our study would aid the interpretation of future influences of Hg originated from bedrock erosion and exposure of terrestrial landscapes.

In addition to the application in the Arctic, reconstruction of atmospheric Hg influence over the Holocene is important in the low-latitude environment, where Hg sourced from precipitation and terrestrial runoff acts as a dominant source to coastal and marine environment in the absence of glacier dynamics.[65,66] Previous studies have reported increased precipitation and monsoon-like climate during the HTM in the Northern Hemisphere but not in the Southern Hemisphere.[67] The strong climatic variability in the middle Holocene is known to have caused dry climate in parts of South America, Asia, and Africa.[67−69] Given the large isotopic difference between precipitation and terrestrial sources,[12] we believe that Hg isotope reconstruction in low-latitude sedimentary archives can be used to resolve the influence of precipitation-derived Hg versus terrestrial runoff of Hg^0 sequestered in foliage and to gain further insights into the Holocene climate variability resulting in such difference. Future utility of Hg isotopes as a climate proxy would benefit from applications in well-established systems, where physical, biogeochemical, and geological changes caused by climate have been assessed and verified in detail. Applications of Hg isotopes for resolving changes in Hg sources spanning longer geological time scales and during well-known climatic events would also increase the utility of Hg isotopes.

■ ASSOCIATED CONTENT

Supporting Information

The Supporting Information is available free of charge at https://pubs.acs.org/doi/10.1021/acsearthspacechem.1c00095.

https://doi.org/10.1021/acsearthspacechem.1c00095
ACS Earth Space Chem. 2021, 5, 2398−2407

Lithology and geological properties of Dicksonfjorden and Woodfjorden bedrocks (Table S1); data sources of the biogeochemical measurements (TOC, $\delta^{13}C$, and ε_{Nd}) of Dicksonfjorden and Woodfjorden sediment cores (Table S2); mercury isotope ratios of the standard reference materials measured in this study (Table S3); THg concentration, TOC, THg/TOC, and Hg isotope ratios of JM05-046-GC (JM05) sediment core (Table S4); THg concentration, TOC, THg/TOC, and Hg isotope ratios of HH12-964-GC (HH12) sediment core (Table S5) (PDF)

AUTHOR INFORMATION

Corresponding Author

Sae Yun Kwon − *Division of Environmental Science and Engineering, Pohang University of Science and Technology, Pohang 37673, South Korea; Institute for Convergence Research and Education in Advanced Technology, Yonsei University, Incheon 21983, South Korea;* orcid.org/0000-0001-8665-0327; Email: saeyunk@postech.ac.kr

Authors

Ju Hyeon Lee − *Division of Environmental Science and Engineering, Pohang University of Science and Technology, Pohang 37673, South Korea;* orcid.org/0000-0001-5070-5074

Hoin Lee − *Division of Environmental Science and Engineering, Pohang University of Science and Technology, Pohang 37673, South Korea*

Seung-Il Nam − *Division of Glacial Environment Research, Korea Polar Research Institute, Incheon 21990, South Korea*

Jung-Hyun Kim − *Division of Glacial Environment Research, Korea Polar Research Institute, Incheon 21990, South Korea*

Young Ji Joo − *Division of Glacial Environment Research, Korea Polar Research Institute, Incheon 21990, South Korea;* Present Address: Department of Earth and Environmental Sciences, Pukyong National University, 45 Yongso-Ro, Nam-Gu, Busan 48513, South Korea

Kwangchul Jang − *Division of Glacial Environment Research, Korea Polar Research Institute, Incheon 21990, South Korea*

Haryun Kim − *East Sea Research Institute, Korea Institute of Ocean Science and Technology, Uljin 36315, South Korea*

Runsheng Yin − *State Key Laboratory of Ore Deposit Geochemistry, Institute of Geochemistry, Chinese Academy of Sciences, Guiyang 550081 Guizhou, China*

Complete contact information is available at: https://pubs.acs.org/10.1021/acsearthspacechem.1c00095

Notes

The authors declare no competing financial interest.

ACKNOWLEDGMENTS

This work was supported by the National Research Foundation of Korea (NRF) grant funded by the Korea Government (MSIT) [Grant Numbers NRF-2019R1F1A1058928, NRF-2021M1A5A1075512, NRF-2021M1A5A1075513]; the Air−sea exchange, sediment methylation, and ecosystem sources of mercury in the Arctic Ocean Project funded by the Korea Government (MOF) [Grant Number 1525011792]; and the Basic Research Program through the NRF funded by the MSIT [Grant Number NRF-2020R1A4A1018818]. The authors kindly acknowledge Dr. K. C. Yoo (KOPRI) and Dr. Matthias Forwick (UiT, Norway) for providing sediment samples taken during the R.V. Jan Mayen in 2005 and the Helmer Hanssen cruise in 2012, respectively, and the captains, crews, and the scientific parties on board during both cruises.

REFERENCES

(1) Mergler, D.; Anderson, H. A.; Chan, L. H. M.; Mahaffey, K. R.; Murray, M.; Sakamoto, M.; Stern, A. H. Methylmercury exposure and health effects in humans: a worldwide concern. *AMBIO* **2007**, *36*, 3−11.

(2) Engstrom, D. R.; Fitzgerald, W. F.; Cooke, C. A.; Lamborg, C. H.; Drevnick, P. E.; Swain, E. B.; Balogh, S. J.; Balcom, P. H. Atmospheric Hg emissions from preindustrial gold and silver extraction in the Americas: A reevaluation from lake-sediment archives. *Environ. Sci. Technol.* **2014**, *48*, 6533−6543.

(3) Fitzgerald, W. F.; Engstrom, D. R.; Lamborg, C. H.; Tseng, C. M.; Balcom, P. H.; Hammerschmidt, C. R. Modern and historic atmospheric mercury fluxes in northern Alaska: global sources and Arctic depletion. *Environ. Sci. Technol.* **2005**, *39*, 557−568.

(4) Schuster, P. F.; Krabbenhoft, D. P.; Naftz, D. L.; Cecil, L. D.; Olson, M. L.; Dewild, J. F.; Susong, D. D.; Green, J. R.; Abbott, M. L. Atmospheric mercury deposition during the last 270 years: a glacial ice core record of natural and anthropogenic sources. *Environ. Sci. Technol.* **2002**, *36*, 2303−2310.

(5) Stern, G. A.; Macdonald, R. W.; Outridge, P. M.; Wilson, S.; Chetelat, J.; Cole, A.; Hintelmann, H.; Loseto, L. L.; Steffen, A.; Wang, F.; Zdanowicz, C. How does climate change influence arctic mercury? *Sci. Total Environ.* **2012**, *414*, 22−42.

(6) Farnsworth, W. R.; Ingólfsson, Ó.; Alexanderson, H.; Allaart, L.; Forwick, M.; Noormets, R.; Retelle, M.; Schomacker, A. Holocene glacial history of Svalbard: Status, perspectives and challenges. *Earth-Sci. Rev.* **2020**, *208*, No. 103249.

(7) Cooke, C. A.; Wolfe, A. P.; Michelutti, N.; Balcom, P. H.; Briner, J. P. A Holocene perspective on algal mercury scavenging to sediments of an arctic lake. *Environ. Sci. Technol.* **2012**, *46*, 7135−7141.

(8) Outridge, P. M.; Sanei, H.; Mustaphi, C. C.; Gajewski, K. Holocene climate change influences on trace metal and organic matter geochemistry in the sediments of an Arctic lake over 7,000 years. *Appl. Geochem.* **2017**, *78*, 35−48.

(9) Cannon, W. F.; Dean, W. E.; Bullock, J. H., Jr. Effects of Holocene climate change on mercury deposition in Elk Lake, Minnesota: The importance of eolian transport in the mercury cycle. *Geology* **2003**, *31*, 187−190.

(10) Gleason, J. D.; Blum, J. D.; Moore, T. C.; Polyak, L.; Jakobsson, M.; Meyers, P. A.; Biswas, A. Sources and cycling of mercury in the paleo Arctic Ocean from Hg stable isotope variations in Eocene and Quaternary sediments. *Geochim. Cosmochim. Acta* **2017**, *197*, 245−262.

(11) Blum, J. D.; Sherman, L. S.; Johnson, M. W. Mercury isotopes in earth and environmental sciences. *Annu. Rev. Earth Planet. Sci.* **2014**, *42*, 249−269.

(12) Kwon, S. Y.; Blum, J. D.; Yin, R.; Tsui, M. T. K.; Yang, Y. H.; Choi, J. W. Mercury stable isotopes for monitoring the effectiveness of the Minamata Convention on Mercury. *Earth-Sci. Rev.* **2020**, *203*, No. 103111.

(13) Bergquist, B. A.; Blum, J. D. Mass-dependent and mass-independent fractionation of Hg isotopes by photo-reduction in aquatic systems. *Science* **2007**, *318*, 417−420.

(14) Cai, H.; Chen, J. Mass-independent fractionation of even mercury isotopes. *Sci. Bull.* **2016**, *61*, 116−124.

(15) Kurz, A. Y.; Blum, J. D.; Washburn, S. J.; Baskaran, M. Changes in the mercury isotopic composition of sediments from a remote alpine lake in Wyoming, USA. *Sci. Total Environ.* **2019**, *669*, 973−982.

(16) Lepak, R. F.; Janssen, S. E.; Engstrom, D. R.; Krabbenhoft, D. P.; Tate, M. T.; Yin, R.; Fitzgerald, W. F.; Nagorski, S. A.; Hurley, J. P. Resolving Atmospheric Mercury Loading and Source Trends from

Isotopic Records of Remote North American Lake Sediments. *Environ. Sci. Technol.* **2020**, *54*, 9325−9333.
(17) Grasby, S. E.; Them, T. R., II; Chen, Z.; Yin, R.; Ardakani, O. H. Mercury as a proxy for volcanic emissions in the geologic record. *Earth-Sci. Rev.* **2019**, *196*, No. 102880.
(18) Shen, J.; Chen, J.; Algeo, T. J.; Yuan, S.; Feng, Q.; Yu, J.; Zhou, L.; O'Connell, B.; Planavsky, N. J. Evidence for a prolonged Permian−Triassic extinction interval from global marine mercury records. *Nat. Commun.* **2019**, *10*, No. 1563.
(19) Wang, X.; Cawood, P. A.; Zhao, H.; Zhao, L.; Grasby, S. E.; Chen, Z. Q.; Zhang, L. Global mercury cycle during the end-Permian mass extinction and subsequent Early Triassic recovery. *Earth Planet. Sci. Lett.* **2019**, *513*, 144−155.
(20) Masbou, J.; Point, D.; Sonke, J. E.; Frappart, F.; Perrot, V.; Amouroux, D.; Richard, P.; Becker, P. R. Hg stable isotope time trend in ringed seals registers decreasing sea ice cover in the Alaskan Arctic. *Environ. Sci. Technol.* **2015**, *49*, 8977−8985.
(21) Yin, R.; Feng, X.; Hurley, J. P.; Krabbenhoft, D. P.; Lepak, R. F.; Kang, S.; Yang, H.; Li, X. Historical records of mercury stable isotopes in sediments of Tibetan lakes. *Sci. Rep.* **2016**, *6*, No. 23332.
(22) Douglas, T. A.; Blum, J. D. Mercury isotopes reveal atmospheric gaseous mercury deposition directly to the Arctic coastal snowpack. *Environ. Sci. Technol. Lett.* **2019**, *6*, 235−242.
(23) Sherman, L. S.; Blum, J. D.; Johnson, K. P.; Keeler, G. J.; Barres, J. A.; Douglas, T. A. Mass-independent fractionation of mercury isotopes in Arctic snow driven by sunlight. *Nat. Geosci.* **2010**, *3*, 173−177.
(24) Zdanowicz, C. M.; Krümmel, E. M.; Poulain, A. J.; Yumvihoze, E.; Chen, J.; Štrok, M.; Scheer, M.; Hintelmann, H. Historical variations of mercury stable isotope ratios in Arctic glacier firn and ice cores. *Global Biogeochem. Cycles* **2016**, *30*, 1324−1347.
(25) Hansen, T. Late Weichselian and Holocene Sedimentary Processes and Glacier Dynamics in Woodfjorden, Bockfjorden and Liefdefjorden, North Spitsbergen. M.S. Thesis, UiT Norges arktiske universitet: Tromsø, Norway, 2014.
(26) Hagen, J. O.; Liestøl, O.; Roland, E.; Jørgensen, T. *Glacier Atlas of Svalbard and Jan Mayen*; Norway: Norwegian Polar Institute: 1993.
(27) Joo, Y. J.; Forwick, M.; Park, K.; Joe, Y.; Son, Y. J.; Nam, S.-I. Holocene environmental changes in Dicksonfjorden, west Spitsbergen, Svalbard. *Polar Res.* **2019**, *38*, 1−14.
(28) Jang, K.; Bayon, G.; Han, Y.; Joo, Y. J.; Kim, J. H.; Ryu, J. S.; Woo, J.; Forwick, M.; Szczuciński, W.; Kim, J. H.; Nam, S. I. Neodymium isotope constraints on chemical weathering and past glacial activity in Svalbard. *Earth Planet. Sci. Lett.* **2020**, *542*, No. 116319.
(29) Joo, Y. J.; Hansen, T.; Forwich, M.; Nam, S.-I. In *Environmental Changes and Depositional Processes in Woodfjorden of Northern Svalbard Since the Last Deglaciation*, Arctic Science Summit Week 2021; Portugal, 2021.
(30) Blum, J. D.; Bergquist, B. A. Reporting of variations in the natural isotopic composition of mercury. *Anal. Bioanal. Chem.* **2007**, *388*, 353−359.
(31) Blum, J. D.; Johnson, M. W. Recent developments in mercury stable isotope analysis. *Rev. Mineral. Geochem.* **2017**, *82*, 733−757.
(32) Foucher, D.; Hintelmann, H.; et al. Tracing mercury contamination from the Idrija mining region (Slovenia) to the Gulf of Trieste using Hg isotope ratio measurements. *Environ. Sci. Technol.* **2009**, *43*, 33−39.
(33) Mil-Homens, M.; Blum, J.; Canário, J.; Caetano, M.; Costa, A. M.; Lebreiro, S. M.; Trancoso, M.; Richter, T.; de Stigter, H.; Johnson, M.; Branco, V.; et al. Tracing anthropogenic Hg and Pb input using stable Hg and Pb isotope ratios in sediments of the central Portuguese Margin. *Chem. Geol.* **2013**, *336*, 62−71.
(34) Khan, A. L.; Dierssen, H.; Schwarz, J. P.; Schmitt, C.; Chlus, A.; Hermanson, M.; Painter, T. H.; McKnight, D. M. Impacts of coal dust from an active mine on the spectral reflectance of Arctic surface snow in Svalbard, Norway. *J. Geophys. Res.* **2017**, *122*, 1767−1778.
(35) Dowdall, M.; Vicat, K.; Frearson, I.; Gerland, S.; Lind, B.; Shaw, G. Assessment of the radiological impacts of historical coal mining operations on the environment of Ny-Ålesund, Svalbard. *J. Environ. Radioact.* **2004**, *71*, 101−114.
(36) Xue, W.; Kwon, S. Y.; Grasby, S. E.; Sunderland, E. M.; Pan, X.; Sun, R.; Zhou, T.; Yan, H.; Yin, R. Anthropogenic influences on mercury in Chinese soil and sediment revealed by relationships with total organic carbon. *Environ. Pollut.* **2019**, *255*, No. 113186.
(37) Grasby, S. E.; Shen, W.; Yin, R.; Gleason, J. D.; Blum, J. D.; Lepak, R. F.; Hurley, J. P.; Beauchamp, B. Isotopic signatures of mercury contamination in latest Permian oceans. *Geology* **2017**, *45*, 55−58.
(38) Schütze, M.; Tserendorj, G.; Pérez-Rodríguez, M.; Rösch, M.; Biester, H. Prediction of Holocene mercury accumulation trends by combining palynological and geochemical records of lake sediments (Black Forest, Germany). *Geosciences* **2018**, *8*, No. 358.
(39) Beal, S. A.; Kelly, M. A.; Stroup, J. S.; Jackson, B. P.; Lowell, T. V.; Tapia, P. M. Natural and anthropogenic variations in atmospheric mercury deposition during the Holocene near Quelccaya Ice Cap, Peru. *Global Biogeochem. Cycles* **2014**, *28*, 437−450.
(40) Wang, X.; Zhong, W.; Li, T.; Quan, M.; Wang, B.; Wei, Z. A 16.2-kyr lacustrine sediment record of mercury deposition in Dahu Swamp, eastern Nanling Mountains, southern China: Analysis of implications for climatic changes. *Quat. Int.* **2021**, *592*, 12−21.
(41) Cossa, D.; Mucci, A.; Guédron, S.; Coquery, M.; Radakovich, O.; Escoube, R.; Campillo, S.; Heussner, S. Mercury accumulation in the sediment of the Western Mediterranean abyssal plain: A reliable archive of the late Holocene. *Geochim. Cosmochim. Acta* **2021**, *309*, 1−15.
(42) Biswas, A.; Blum, J. D.; Bergquist, B. A.; Keeler, G. J.; Xie, Z. Natural mercury isotope variation in coal deposits and organic soils. *Environ. Sci. Technol.* **2008**, *42*, 8303−8309.
(43) Smith, C. N.; Kesler, S. E.; Blum, J. D.; Rytuba, J. J. Isotope geochemistry of mercury in source rocks, mineral deposits and spring deposits of the California coast ranges, USA. *Earth Planet. Sci. Lett.* **2008**, *269*, 399−407.
(44) Yin, R.; Feng, X.; Li, X.; Yu, B.; Du, B. Trends and advances in mercury stable isotopes as a geochemical tracer. *Trends Environ. Anal. Chem.* **2014**, *2*, 1−10.
(45) Donovan, P. M.; Blum, J. D.; Yee, D.; Gehrke, G. E.; Singer, M. B. An isotopic record of mercury in San Francisco Bay sediment. *Chem. Geol.* **2013**, *349*−*350*, 87−98.
(46) Gehrke, G. E.; Blum, J. D.; Meyers, P. A. The geochemical behavior and isotopic composition of Hg in a mid-Pleistocene western Mediterranean sapropel. *Geochim. Cosmochim. Acta* **2009**, *73*, 1651−1665.
(47) Demers, J. D.; Blum, J. D.; Zak, D. R. Mercury isotopes in a forested ecosystem: implications for air-surface exchange dynamics and the global mercury cycle. *Global Biogeochem. Cycles* **2013**, *27*, 222−238.
(48) Gratz, L. E.; Keeler, G. J.; Blum, J. D.; Sherman, L. S. (2010). Isotopic composition and fractionation of mercury in Great Lakes precipitation and ambient air. *Environ. Sci. Technol.* **2010**, *44*, 7764−7770.
(49) Sherman, L. S.; Blum, J. D.; Dvonch, J. T.; Gratz, L. E.; Landis, M. S. The use of Pb, Sr, and Hg isotopes in Great Lakes precipitation as a tool for pollution source attribution. *Sci. Total Environ.* **2015**, *502*, 362−374.
(50) Yuan, S.; Zhang, Y.; Chen, J.; Kang, S.; Zhang, J.; Feng, X.; Cai, H.; Wang, Z.; Wang, Z.; Huang, Q. Large variation of mercury isotope composition during a single precipitation event at Lhasa City, Tibetan Plateau, China. *Procedia. Earth Planet. Sci.* **2015**, *13*, 282−286.
(51) Jiskra, M.; Wiederhold, J. G.; Skyllberg, U.; Kronberg, R. M.; Kretzschmar, R. Source tracing of natural organic matter bound mercury in boreal forest runoff with mercury stable isotopes. *Environ. Sci.: Processes Impacts* **2017**, *19*, 1235−1248.
(52) Li, C.; Sonke, J. E.; Le Roux, G.; Piotrowska, N.; Van der Putten, N.; Roberts, S. J.; Daley, T.; Rice, E.; Gehrels, R.; Enrico, M.; Mauquoy, D.; Roland, T. P.; De Vleeschouwer, F. Unequal anthropogenic enrichment of mercury in Earth's northern and southern hemispheres. *ACS Earth Space Chem.* **2020**, *4*, 2073−2081.

https://doi.org/10.1021/acsearthspacechem.1c00095
ACS Earth Space Chem. 2021, 5, 2398−2407

(53) Enrico, M.; Le Roux, G.; Heimbürger, L. E.; Van Beek, P.; Souhaut, M.; Chmeleff, J.; Sonke, J. E. Holocene atmospheric mercury levels reconstructed from peat bog mercury stable isotopes. *Environ. Sci. Technol.* **2017**, *51*, 5899−5906.
(54) Wang, X.; Luo, J.; Yin, R.; Yuan, W.; Lin, C. J.; Sommar, J.; Feng, X.; Wang, H.; Lin, C. Using mercury isotopes to understand mercury accumulation in the montane forest floor of the Eastern Tibetan Plateau. *Environ. Sci. Technol.* **2017**, *51*, 801−809.
(55) Kim, H.; Kwon, S. Y.; Lee, K.; Lim, D.; Han, S.; Kim, T. W.; Joo, Y. J.; Lim, J.; Kang, M. H.; Nam, S. I. Input of terrestrial organic matter linked to deglaciation increased mercury transport to the Svalbard fjords. *Sci. Rep.* **2020**, *10*, No. 3446.
(56) Miller, G. H.; Landvik, J. Y.; Lehman, S. J.; Southon, J. R. Episodic Neoglacial snowline descent and glacier expansion on Svalbard reconstructed from the 14C ages of ice-entombed plants. *Quat. Sci. Rev.* **2017**, *155*, 67−78.
(57) Funder, S.; Goosse, H.; Jepsen, H.; Kaas, E.; Kjær, K. H.; Korsgaard, N. J.; Larsen, N. K.; Linderson, H.; Lyså, A.; Möller, P.; Olsen, J.; Willerslev, E. A 10,000-Year Record of Arctic Ocean Sea-Ice Variability—View from the Beach. *Science* **2011**, *333*, 747−750.
(58) Mann, M. E.; Zhang, Z.; Rutherford, S.; Bradley, R. S.; Hughes, M. K.; Shindell, D.; Ammann, C.; Faluvegi, G.; Ni, F. Global signatures and dynamical origins of the Little Ice Age and Medieval Climate Anomaly. *Science* **2009**, *326*, 1256−1260.
(59) Bartels, M.; Titschack, J.; Fahl, K.; Stein, R.; Seidenkrantz, M.-S.; Hillaire-Marcel, C.; Hebbeln, D. Atlantic Water advection vs. glacier dynamics in northern Spitsbergen since early deglaciation. *Clim. Past* **2017**, *13*, 1717−1749.
(60) Motta, L. C.; Blum, J. D.; Johnson, M. W.; Umhau, B. P.; Popp, B. N.; Washburn, S. J.; Drazen, J. C.; Benitez-Nelson, C. R.; Hannides, C. C. S.; Close, H. G.; Lamborg, C. H. Mercury cycling in the North Pacific Subtropical Gyre as revealed by mercury stable isotope ratios. *Global Biogeochem. Cycles* **2019**, *33*, 777−794.
(61) Streets, D. G.; Horowitz, H. M.; Jacob, D. J.; Lu, Z.; Levin, L.; Ter Schure, A. F.; Sunderland, E. M. Total mercury released to the environment by human activities. *Environ. Sci. Technol.* **2017**, *51*, 5969−5977.
(62) Sun, R.; Jiskra, M.; Amos, H. M.; Zhang, Y.; Sunderland, E. M.; Sonke, J. E. Modelling the mercury stable isotope distribution of Earth surface reservoirs: Implications for global Hg cycling. *Geochim. Cosmochim. Acta* **2019**, *246*, 156−173.
(63) Cooke, C. A.; Hintelmann, H.; Ague, J. J.; Burger, R.; Biester, H.; Sachs, J. P.; Engstrom, D. R. Use and legacy of mercury in the Andes. *Environ. Sci. Technol.* **2013**, *47*, 4181−4188.
(64) Meredith, M.; Sommerkorn, M.; Cassotta, S.; Derksen, C.; Ekaykin, A.; Hollowed, A.; Kofinas, G.; Mackintosh, A.; Melbourne-Thomas, J.; Muelbert, M. M. C.; Ottersen, G.; Pritchard, H.; Schuur, E. A. G. Polar Regions. In *IPCC Special Report on the Ocean and Cryosphere in a Changing Climate*; Pörtner, H.-O.; Roberts, D. C.; Masson-Delmotte, V.; Zhai, P.; Tignor, M.; Poloczanska, E.; Mintenbeck, K.; Alegría, A.; Nicolai, M.; Okem, A.; Petzold, J.; Rama, B.; Weyer, N. M., Eds.; Intergovernmental Panel on Climate Change, 2019; pp 203−320.
(65) Balcom, P. H.; Fitzgerald, W. F.; Vandal, G. M.; Lamborg, C. H.; Rolfhus, K. R.; Langer, C. S.; Hammerschmidt, C. R. Mercury sources and cycling in the Connecticut River and Long Island Sound. *Mar. Chem.* **2004**, *90*, 53−74.
(66) Mason, R. P.; Lawson, N. M.; Lawrence, A. L.; Leaner, J. J.; Lee, J. G.; Sheu, G. R. Mercury in the Chesapeake Bay. *Mar. Chem.* **1999**, *65*, 77−96.
(67) An, S. I.; Im, S. H.; Jun, S. Y. Changes in ENSO activity during the Last 6,000 Years Modulated by Background Climate State. *Geophys. Res. Lett.* **2018**, *45*, 2467−2475.
(68) Haug, G. H.; Hughen, K. A.; Sigman, D. M.; Peterson, L. C.; Röhl, U. Southward migration of the intertropical convergence zone through the Holocene. *Science* **2001**, *293*, 1304−1308.
(69) Wang, Y.; Cheng, H.; Edwards, R. L.; He, Y.; Kong, X.; An, Z.; Wu, J.; Kelly, M. J.; Dykoski, C. A.; Li, X. The Holocene Asian Monsoon: Links to Solar Changes and North Atlantic Climate. *Science* **2005**, *308*, 854−857.

https://doi.org/10.1021/acsearthspacechem.1c00095
ACS Earth Space Chem. 2021, 5, 2398−2407